

# Quantile Mapping Bias Correction on Rossby Centre Regional Climate Models for Precipitation Analysis over Kenya, East Africa

Brian Ayugi<sup>1</sup>, Guirong Tan<sup>1\*</sup>, Rouyun Niu<sup>2</sup>, Hassen Babaousmail<sup>1,3</sup>, Moses Ojara<sup>1,4</sup>, Hanggoro Wido<sup>1,5</sup>, Lucia Mumo<sup>1</sup>, Isaac Kwesi Noon<sup>1,6</sup>, Victor Ongoma<sup>1,7</sup>

<sup>1</sup>Key Laboratory of Meteorological Disaster, Ministry of Education (KLME)/Joint International Research Laboratory of Climate and Environment Change (ILCEC)/Collaborative Innovation Center on Forecast and Evaluation of Meteorological Disasters (CIC-FEMD), Nanjing, University of Information Science and Technology, Nanjing 210044, China

<sup>2</sup>National Meteorological Center, China Meteorological Administration, Beijing 100081, China

<sup>3</sup>School of Computer and Software, Nanjing University of Information Science and Technology, Jiangsu, Nanjing 210044, China

<sup>4</sup>Uganda National Meteorological Authority, Clement Hill Road, P.O. Box 7025 Kampala, Uganda

<sup>5</sup>Research and Development Center of Indonesia Agency for Meteorology Climatology and Geophysics, Jakarta, Indonesia, 10720

<sup>6</sup>School of Geographical Sciences, Nanjing University of Information Science and Technology, Nanjing 210044, China

<sup>7</sup>School of Geography, Earth Science and Environment, University of the South Pacific, Laucala Campus Private Bag, Suva, Fiji

\*Email: [tanguirong@nuist.edu.cn](mailto:tanguirong@nuist.edu.cn)

## Abstract

Accurate assessment and projections of extreme climate events requires the use of climate datasets with no or minimal error. This study uses quantile mapping bias correction (QMBC) method to correct the bias of five Regional Climate Models (RCMs) from the latest output of Rossby Climate Model Center (RCA4) over Kenya, East Africa. The outputs were validated using various scalar metrics such as Root Mean Square Difference (RMSD), Mean Absolute Error (MAE) and mean Bias. The study found that the QMBC algorithm demonstrate varying performance among the models in the study domain. The results show that most of the models exhibit significant improvement after corrections at seasonal and annual timescales. Specifically, the European community Earth-System (EC-EARTH) and Commonwealth Scientific and Industrial Research Organization (CSIRO) models depict exemplary improvement as compared to other models. On the contrary, the Institute Pierre Simon Laplace Model CM5A-MR (IPSL-CM5A-MR) model show little improvement across various timescales (i.e. March-April-May (MAM) and October-November-December (OND)). The projections forced with bias corrected historical simulations tallied observed

39 values demonstrate satisfactory simulations as compared to the uncorrected RCMs output  
40 models. This study has demonstrated that using QMBC on outputs from RCA4 is an  
41 important intermediate step to improve climate data prior to performing any regional impact  
42 analysis. The corrected models can be used for projections of drought and flood extreme  
43 events over the study area. This study analysis is crucial from the sustainable planning for  
44 adaptation and mitigation of climate change and disaster risk reduction perspective.

45 **Keywords:** Quantile Mapping Bias Correction (QMBC), Regional Climate Models (RCMs),  
46 Rossby Centre Regional Climate Models (RCA4), Drought, Flood, Kenya

## 47 1. Introduction

48 Recently, the changes in the frequency and intensity of extreme events have led to  
49 serious climate related disasters across many parts of the world. These extreme events (i.e.  
50 floods, droughts, and/or heatwaves) have gained considerable attention by climate scientists  
51 and the general public due their devastating impact on ecosystem and different sectors of the  
52 society.

53 Thus, monitoring and forecasting of such extreme events is crucial steps to ensure that  
54 the Malabo Goals 2025 and the 2030 Agenda for Sustainable Development of the Sustainable  
55 Development Goal 2 (SDG2) are met ([FAO, 2019](#)). It is against this backdrop that climate  
56 information's availability and accuracy are important for climate change assessment ([IPCC,](#)  
57 [2014](#)).

58 From a policy formulation perspective, global climate models (GCMs) and regional  
59 climate models (RCMs) are such examples of datasets used in forecasting and projecting  
60 studies. Additionally, model outputs from GCMs and RCMs are sometimes used as input data  
61 source in the forecasting and projection of the extreme events. However, these model outputs  
62 are saddled with uncertainties that arise due to systematic and/or random biases relative to in-  
63 situ datasets ([Christensen et al., 2008](#); [Teutschbein and Seibert, 2010](#)). For example, [Cardell](#)  
64 [et al., \(2019\)](#) associated the model random error to intricate topography or atmosphere-  
65 biosphere transition along large water bodies. In a different study, [Allen et al., \(2006\)](#) linked  
66 systematic errors (model biases) to model coarser resolutions or parameterizations schemes.

67 Other studies (e.g., [Mearns et al., 2012](#); [Cannon et al., 2015](#)), also reported  
68 considerable deviations (i.e. over/underestimations) relative to in-situ observations. Thus,  
69 within the context of these studies, readers are cautioned when generalizing results from these  
70 models outputs. Of great interest, are water resource planners and managers, who are required

71 to periodically conduct regional impact analysis to assess the impacts of climate change on  
72 watershed hydrology. Thus, to quantify the changes and predict extreme events against the  
73 backdrop of warming climate, scientists and policy analyst alike have no option than to use  
74 the existing GCM and RCM ensembles, despite report of uncertainties in their climate change  
75 assessment (IPCC, 2014).

76 Meanwhile, different spatial downscaling and bias correction tools have been  
77 proposed and applied extensively to remove this inherent errors or biases. Thus, to correct or  
78 minimize these biases or errors, scientists use two distinct spatial downscaling and bias  
79 correction tools; namely, statistical and dynamic downscaling methods.

80 In this study, we do not attempt to compare the advantages and disadvantages of these  
81 methods since extensive literature review concludes that it is difficult to define the best  
82 method as the overall output performance of the two methods are able to reproduce the recent  
83 climate (Murphy, 1999; Wilby and Wigley., 2000; Ahmad et al., 2013). From literature, these  
84 two methods have been applied to downscale GCM to RCM (IPCC, 2014).

85 Several RCMs based on dynamic downscaling are now available for many regions  
86 across the globe (IPCC, 2014). Example includes the RCM precipitation data sourced from  
87 Rossby Centre Climate Model outputs (Samuelsson et al., 2012; Strandberget al., 2014).  
88 However, following a phenomenal study of Ahmed et al., (2013) and Wood et al. (2004), it is  
89 clear that the spatial resolution of the RCM for regional or local applications, may not be high  
90 enough and/or still contain some inherent errors. To use this type of climate data for present  
91 and future climate predictions, the two studies recommended bias corrections of RCM data to  
92 remove possibly the biases prior to their application. In parallel, this is particularly relevant  
93 for the Africa continent as well as her sub-regions where the number of in-situ stations, data  
94 availability, and quality have considerably declined and become less reliable (Malhi and  
95 Wright (2004).

96 Thus, to remove biases in RCM, recent studies (Christensen et al., 2008; Terink et al.,  
97 2008; Teutschbein and Seibert, 2012; Fang et al., 2015; Cardell et al., 2019) have adopted  
98 statistical technique to adjust RCMs simulations and projections of climatic variables using  
99 different bias correction methods.

100 Examples of the bias correction methods include the delta correction (Moore et al.,  
101 2008; Rasmussen et al., 2012); Linear transformation (Lenderink et al., 2007); Local Intensity  
102 Scaling (Schmidli et al., 2006); Power Transformation (Leander et al., 2008); Distribution  
103 mapping (Block et al., 2009; Sun et al., 2011); and the Quantile Mapping Bias Correction

104 (QMBC) (Panofsky and Brier, 1968; Piani et al., 2009; Themeßl et al., 2011), just to mention  
105 a few.

106 The conclusions drawn from these studies suggest that QMBC algorithm outperform  
107 other methods (Gudmundsson et al., 2012; Teutschbein and Seibert, 2012; Chen et al., 2013).  
108 It is important to note that QMBC is also referred as quantile-quantile mapping (Sun et al.,  
109 2011), probability mapping (Ines and Hansen, 2006), statistical downscaling (Piani et al.,  
110 2010), or histogram equalization (Rojas et al., 2011).

111 The QMBC method is based on the hypothesis that climate biases that need to be  
112 corrected are unchanging hence its features in historical data will persist into the future  
113 projections (Maraun et al., 2010, 2012). Although, this study acknowledges that QMBC  
114 technique has limitations (see Boé et al., 2007; Cannon et al., 2015), QMBC usage is widely  
115 preferred for impact analysis (Maraun, 2013; Hempel et al., 2013; Maurer and Pierce, 2014;  
116 Cannon et al., 2015).

117 Over the East Africa region, recent studies have reported existence of biases in RCMs  
118 and GCMs datasets (Endris et al., 2013; Kisembe et al., 2018; Ongoma et al., 2019). To  
119 illustrate, Ayugi et al. (2020) demonstrated the manifestation of systematic dry (wet) biases  
120 over regions of low (high) altitude characterized by arid and semi-arid lands (ASALs) or  
121 complex topography. Furthermore, the study highlighted that most mean spatial biases tend to  
122 follow the physiographic features in the study domain, which RCMs could not clearly  
123 reproduce due to its coarser resolution (~50 km) and physical parameterization.

124 Despite the observed biases, few studies have attempted to correct systematic  
125 distributional biases relative to historical observations, and possible future simulations on the  
126 RCMs or GCMs. A number of studies have however improved the quality of satellite-derived  
127 estimates using other techniques, such as Bayesian approach (Kimani et al., 2018a,b).

128 In order to improve the accuracy of projections of extreme events such as drought and  
129 flood over East Africa, better performing RCMs and satellite datasets (Endris et al., 2013;  
130 Kimani et al., 2018a, b; Ayugi et al., 2019, 2020) ought to be further improved using  
131 correctional techniques so as to minimize possible biases and enhance the quality (Maraun et  
132 al., 2010).

133 Thus, as a follow-up from Ayugi et al. (2020), this study focuses on assessing the  
134 importance and performance of QMBC on model outputs over East Africa as an intermediate  
135 step prior to performing any regional impact analysis. This analysis is crucial from the  
136 sustainable planning for adaptation and mitigation of climate change and disaster risk  
137 reduction perspective. The objective of this study is to perform bias correction on the RCMs

138 over Kenya, using QMBC prior to the assessment and projections of floods and droughts in  
139 the mentioned study domain.

140 The remaining section of the paper are organized as follows: Section 2 highlights data  
141 and methods used whilst results and discussions are presented in section 3. The last sections  
142 summarize conclusion of the study with possible recommendation.

143

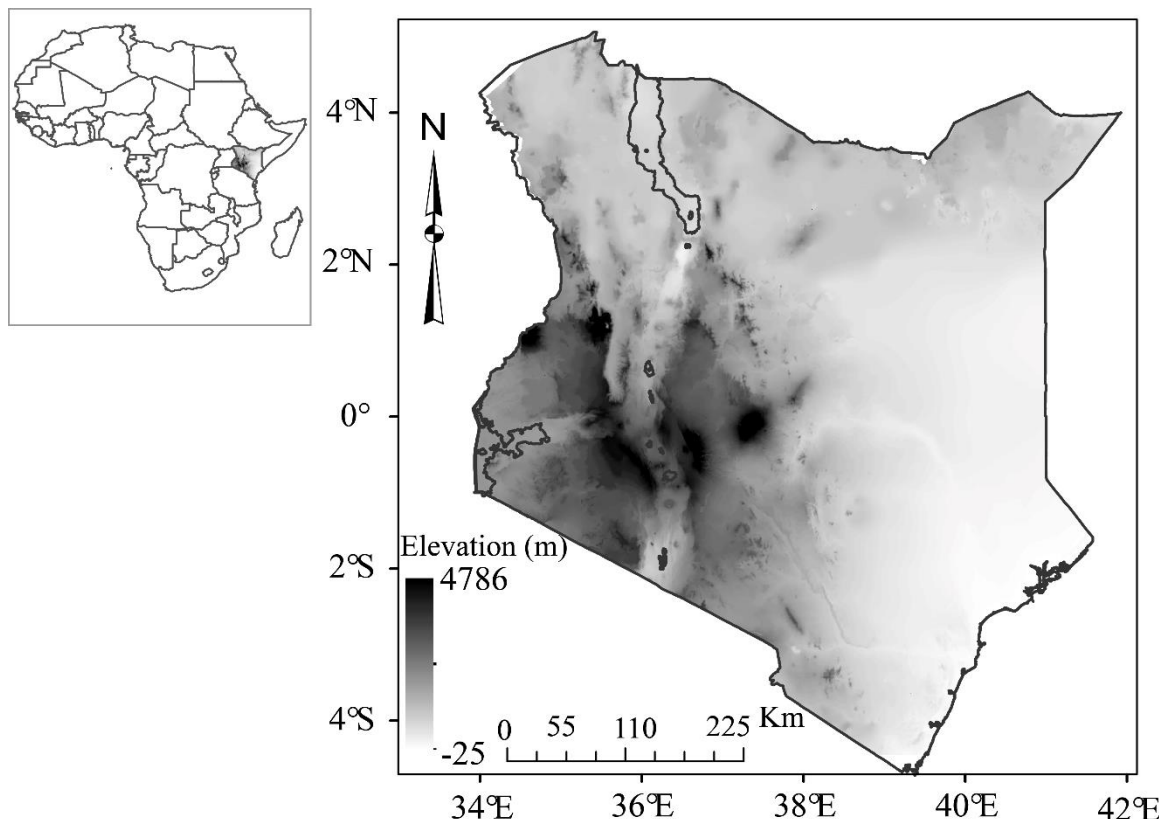
## 144 **2. Study Area, Data and Techniques**

145 **2.1 Study Area**

146 The region under study is situated in East Africa located along the celestial longitude 34° E-  
147 42° E and latitude 5° S - 5° N (**Figure 1**). Diverse physical features that play significant role  
148 in climate modulation from one locality to another characterize this region (Bowen et al.,  
149 2007). For instance, the maximum thermal heat evidenced over the eastern and northeast  
150 parts that are predominantly Arid and Semi-Arid Lands (ASALs) and minimum temperatures  
151 over central regions is due to high elevation point. Moreover, the uppermost (lowest)  
152 elevation with altitude (>5000 m/<0 m) often leads to random uncertainties in climatic  
153 variables during the quantification process (Allen et al., 2006). Consequently, the terrestrial  
154 heterogeneous classification influences socio-economic activity with a great inclination to  
155 rain fed agriculture (Mumo et al., 2018).

156 Meanwhile, the region is classified as tropical climate (Kottek et al., 2006) with  
157 bimodal patterns of rainfall is experienced during March to May (MAM) and October to  
158 December (OND) (Ongoma and Chen, 2017; Ayugi et al., 2019). Looking more closely at the  
159 two seasons, the months of May and November record the highest amount of rainfall across  
160 the study domain whilst March and October signify the onset of the seasons and record the  
161 least rainfall quantity (Ayugi et al., 2016, 2018; Ongoma and Chen., 2017; Mumo et al.,  
162 2019).

163 On the other hand, the highest temperature climatology is observed during January  
164 and February (JF) whereas lowest is observed during June to September (JJAS) (Kinguyu et  
165 al., 2000; Ongoma et al., 2017; Ayugi and Tan, 2019). Generally, microclimate features over  
166 the study area is mostly regulated by the existence of unique geomorphology while synoptic  
167 features are influenced by interaction between atmosphere and hydrosphere within the lower  
168 troposphere. For example, the changes in Hadley circulation which has an influence in the  
169 oscillation of Inter tropical convergence zone (ITCZ), strongly regulate seasonal climate  
170 patterns over the study domain (Nicholson, 2008; Hastenrath et al., 2011).



171

172 **Fig. 1** The study area [34°E–42°E and 5°S–5°N ] with topographical elevation (m) in dark  
 173 color. Enclosed is map of African domain with study domain situated in Eastern region  
 174 marked with dark color.

175

## 176 **2.3 Data and Techniques**

### 177 *2.3.1 Bias correction method*

178 Biases in climate model simulation are commonly detected by validation, (i.e. comparison  
 179 with observation) through computational of mean, or/and other complex analysis  
 180 (Teutschbein and Seibert, 2013). A number of correction techniques have been proposed to  
 181 rectify the existing biases in climate datasets (Lenderink et al., 2007; Leander et al., 2008;  
 182 Moore et al., 2008; Sun et al., 2011).

183 The current study employed QMBC algorithm to evaluate monthly RCMs  
 184 precipitation data sourced from Rossby Centre Climate Model outputs (Samuelsson et al.,  
 185 2012; Strandberget al., 2014) and their respective Mean Multi-model Ensemble (MME).  
 186 They are as follows: Model for Interdisciplinary Research on Climate (MIROC5),  
 187 Commonwealth Scientific and Industrial Research Organization (CSIRO), Institute Pierre  
 188 Simon Laplace Model CM5A-MR (IPSL-CM5A-MR), Max Planck Institute Earth System  
 189 Model at base resolution (MPI-ESM-LR) and European community Earth-System (EC-

190 EARTH). The RCMs have spatial resolution of resolution of  $0.44^\circ \times 0.44^\circ$  ( $\sim 50 \times 50$  km)  
191 with a historical coverage spanning from 1951 to 2005 for the simulations run whilst  
192 projections has temporal span from 2006 to 2100 for both RCP 4.5 and 8.5. The datasets were  
193 retrieved from Deutsches Klimarechenzentrum GmbH (DRKZ) website ([CERA-WDCC](https://cera-www.dkrz.de),  
194 <https://cera-www.dkrz.de>).

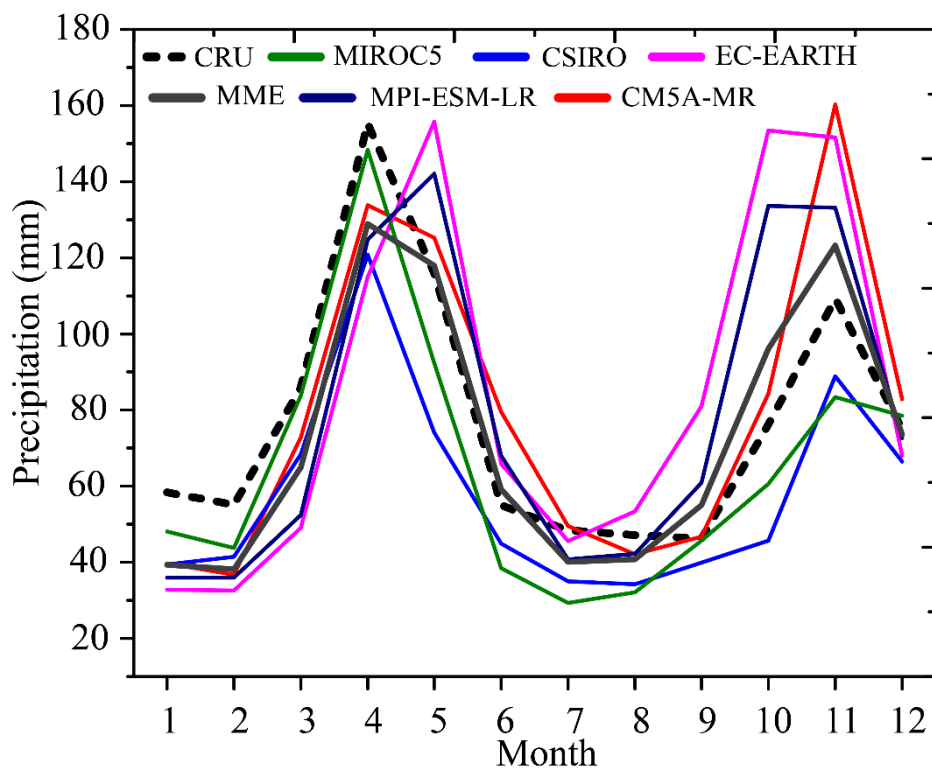
195 Recent version Climatic Research Unit (CRU TS4.02) datasets were employed as  
196 observed datasets during the validation period. [Harris et al. \(2014\)](#) detailed more on this  
197 dataset. The CRU datasets utilized in this study has temporal scale ranging from 1901-2017  
198 and spatial coverage of  $\sim 50$  km. The RCMs datasets were evaluated in a recent study ([Ayugi  
199 et al., 2020](#)) and elucidated the listed models as better performing from the ten GCMs that  
200 were dynamically downscaled based on RCA4 model. Despite the skillful simulation of  
201 observed rainfall as compared to other models, the datasets still reported glaring biases  
202 ([Figure 2; Ayugi et al., 2020](#)). Most models exhibit the overestimation during OND season  
203 and underestimation throughout MAM season ([Figure 2](#)). This has prompted the need for  
204 minimizing the biases in order to employ the models for drought and flood projections in a  
205 region that is vulnerable to occurrence of extreme events.

206 The QMBC constructs cumulative distribution functions (CDFs) of the model and  
207 observations using a transfer function, which in turn translates the raw model outputs into  
208 corrected output. Thus, the CDF of the corrected model are transformed to match that of the  
209 observed datasets ([Piani et al., 2009; Sun et al., 2011; Deutschbein and Seibert, 2012](#)).  
210 Mathematically, quantile mapping is constructed using Eqn 1;

$$y = F_{obs}^{-1}(F_{RCM}(x)) \quad (1)$$

211  
212 where  $y$  is the corrected rainfall value, while  $x$  is the value of precipitation to be corrected. On  
213 the other hand,  $F_{obs}^{-1}$  is the inverse of the CDF of the observation and  $F_{RCM}$  is the CDF of the  
214 RCM employed. The likelihood of detecting  $x$  (mm/month) or less in the model is then  
215 transferred to the quantile of the observed CDF, matching very similar to observed  
216 probability. The QMBC was conducted using available *qmap* package on the R software  
217 ([Gudmundsson et al., 2012](#)).

218



219

220 **Fig. 2** Monthly precipitation for the period 1951-2005 as simulated by 5 individual models of  
 221 RCA4 over Kenya, depicting underestimation or overestimation of observed precipitation.  
 222 Observations (black dotted line) and RCMs Multi-Model Mean (MME) ensemble (gray line)  
 223 are displayed as well.

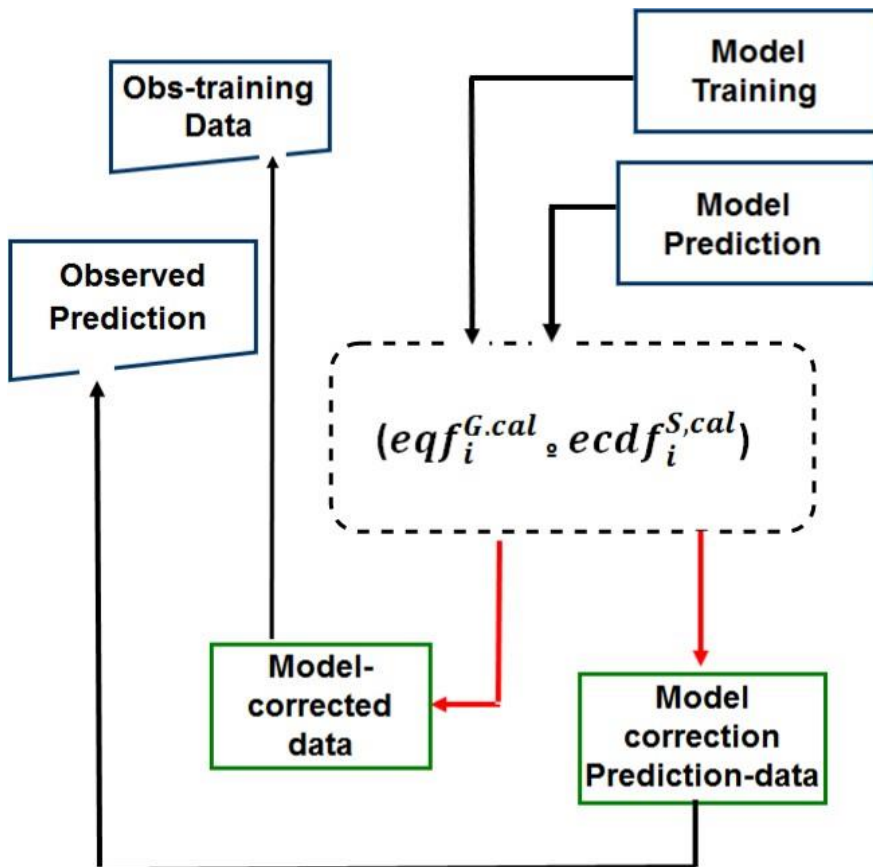
224

225 *2.3.2 Testing the reliability of model correction approach*

226 A number of approaches are utilized in a bid to affirm the reliability of the model correction  
 227 approach. The present study uses a split sample testing (SST) to examine how effective  
 228 QMBC algorithm work under different conditions. More information regarding this approach  
 229 is presented in [Klemeš \(1986\)](#). Meanwhile, SST technique involves splitting the data into two,  
 230 preferably equal size segment in order to use one as calibration and the one for validation.

231 In the current study, the SST approach was conducted by first training data for 29  
 232 years, (1951-1979), to derive biases field for monthly averages in model and observed  
 233 precipitation simulations. The monthly biased field were then used to correct independent  
 234 RCMs during the next 26-year validation period (1980-2005). Additionally, projections  
 235 estimates were corrected for the whole period, i.e., 2006-2100. The hypothesis for SST  
 236 technique is the temporal consistency of average errors. **Figure 3** shows a summary flow of  
 237 the SST approach used in this study.

238



239

240 **Fig. 3** Flowchart of model bias correction procedure

241

242 *2.3.3 Evaluation of bias correction approach*

243 Evaluation of bias corrected RCMs; historical simulations, and projection estimates was  
 244 conducted using raw and bias corrected RCMs related to the observed gridded precipitation  
 245 datasets on monthly and year basis. Statistical metrics such as the Mean Bias, Mean Absolute  
 246 Error (MAE), and customized RMSE to a space and time scenario, were employed to  
 247 compute their relationships. The mathematical formulas of the aforementioned metrics are  
 248 given in Eqns 2 – 4;

$$BIAS = n^{-1} \sum_{i=1}^n (M_i - O_i) \quad (2)$$

$$MAE = n^{-1} \sum_{k=1}^n |P_{M_k} - P_{R_k}| \quad (3)$$

$$RMSE = \sqrt{n^{-1} \sum_{i=1}^n (P_{M_k} - P_{R_k})^2} \quad (4)$$

249

250 where  $P_{M_k}$  is the model estimate for the considered data point  $k$ .  $P_{R_k}$  is the observed value for  
 251 the considered data point  $k$ , and  $N$  is the length of the distribution of the data point being  
 252 analyzed. For graphical displays, the study used Empirical quantile mapping distribution  
 253 (ECDF) and spatial maps to demonstrate the effectiveness of QMBC algorithm.

254 **3. Results and Discussions**

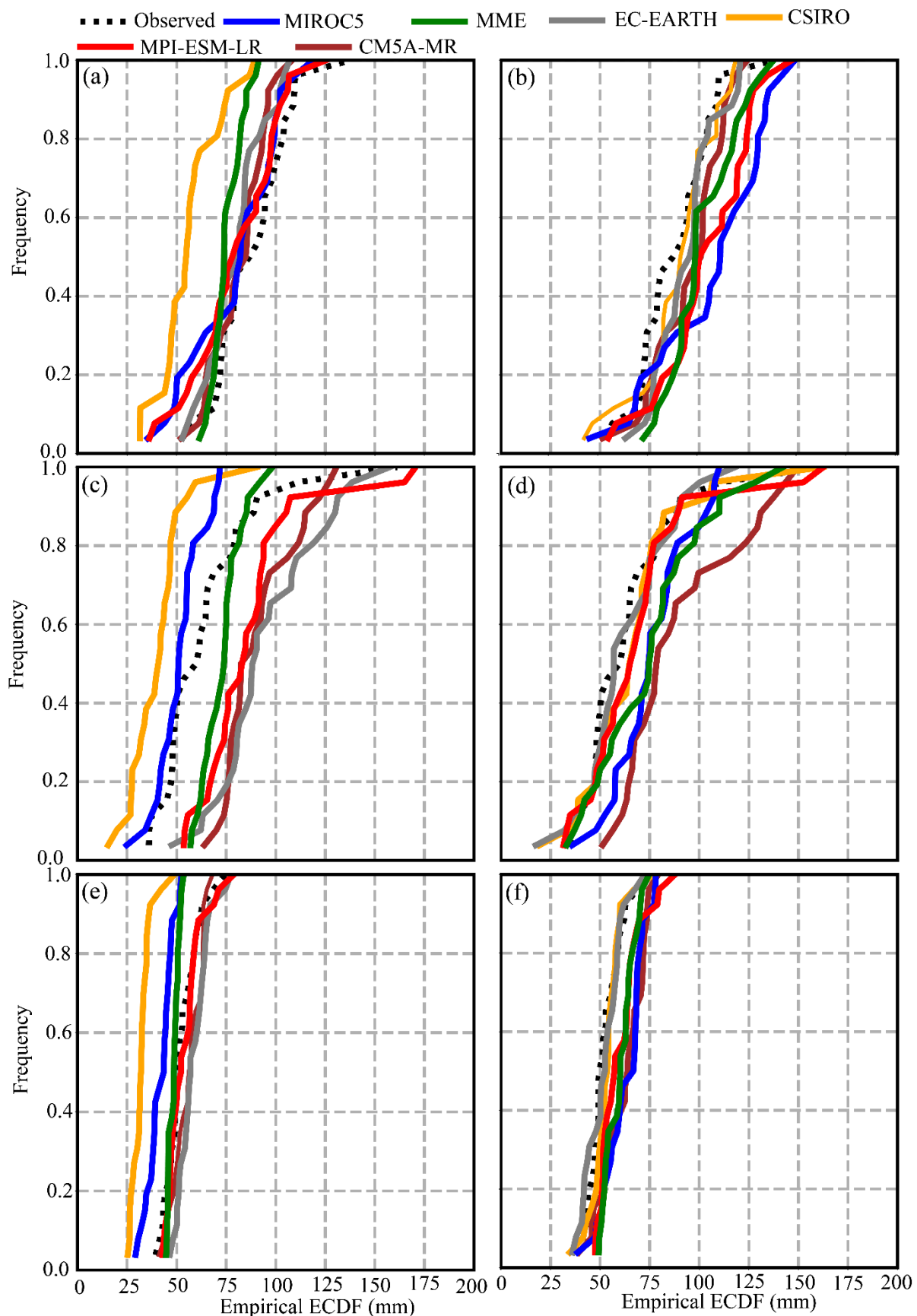
255 *3.1 Evaluation of Bias-corrected RCMs Simulations.*

257 *3.1.1 Temporal assessment*

258 **Figure 4** presents ECDF analysis for 5 GCMs dynamically downscaled with the Rossby  
 259 Centre Regional Climate Model (RCA4), as well as their ensemble average. The plots (a-b)  
 260 represent March-May (MAM) season, (c-d) October-December (OND), and (e-f) annual  
 261 before and after corrections, abbreviated with ‘BC’ and ‘AC’, respectively. The MAM period  
 262 experiences substantial amount of rainfall in terms of magnitude, intensity and frequency,  
 263 thereby exhibiting large biases (Yang et al., 2015; Nicholson et al., 2017). The observed  
 264 biases were noted from a recent studies (Endris et al., 2013; Ayugi et al., 2020) that evaluated  
 265 the performance of RCMs in simulating precipitation climatology over the Great Horn of  
 266 Africa domain. The aforementioned studies demonstrated the under/overestimations of MAM  
 267 rainfall in regions mostly associated with complex physiographical features. Compared to the  
 268 observed datasets (CRU TS4.02; dotted line in Figure 4), it is apparent that QMBC technique  
 269 significantly improved the accuracy of most models and their ensemble after the corrections.  
 270 Specifically, there was a remarkable reduction in Mean Bias, RMSD and MAE in most  
 271 models with significant performance depicted during May (**Table 1**).

272 Majority of the models show insignificant improvement after correction during MAM.  
 273 For example, the mean absolute error (MAE) was generally large in MME-AC (24  
 274 mm/month) as compared to MME-BC (18.77 mm/month) (**Table 1**). Interestingly, CSIRO  
 275 and EC-EARTH show a remarkable enhancement during the wet months as compared to  
 276 other models that exhibited variations from one month to another. Overly, these results show  
 277 that the algorithm improved the model accuracy despite the noteworthy variation based on  
 278 the magnitude of rainfall experienced over the study domain. For instance, there are large

279 incidences of biases noted in May as compared to model underestimations during March and  
 280 April.



281

282 **Fig. 4** The ECDF plots for 5 GCMs dynamically downscaled with the Rossby Centre  
 283 Regional Climate Model (RCA4), as well as their ensemble average. The plots (a-b) represent  
 284 March-May (MAM) season, (c-d) October-December (OND), and (e-f) annual before and  
 285 after corrections.

286

287 In OND season (**Figure 4c-d**), a number of models show large biases before  
 288 corrections that are mostly associated with orographic processes and related teleconnections  
 289 thus influencing rainfall variability and trends (Camberlin and Okoola, 2003; Ogwang et al.,  
 290 2014). Most biases increased with increase in rainfall magnitude with some models  
 291 exhibiting considerable biases even after correction (**Figure 4c-d and Table 1**). In general,  
 292 the results of this analysis show consistent notable improvement by most models during OND  
 293 season.

294

295 **Table 1.** Comparison of different RCMs using summary statistics against the observed data for the validation.  
 296 The effect of bias correction on other statistics (Correlation coefficient), in this case, very small, and the results  
 297 not reported.

RCMs validation							
	RCMs	Mean Bias	Bias (bc)	RMSD	RMSD (bc)	MAE	MAE (bc)
MAM	CM5A-MR	6.52	-8.54	24.38	27.84	20.95	22.42
	CSIRO	31.98	-2.58	40.20	26.93	32.75	22.16
	EC-EARTH	8.57	-6.04	25.33	25.11	18.46	16.96
	MIROC5	8.48	-17.31	29.21	47.51	24.21	37.61
	MPI-ESM-LR	8.11	19.66	28.75	36.20	20.94	29.98
OND	MME	12.73	-16.28	23.61	31.12	18.77	24.37
	CM5A-MR	-26.68	-27.32	38.11	46.49	31.86	36.77
	CSIRO	24.23	0.53	38.22	40.82	27.92	28.38
	EC-EARTH	-31.01	2.90	47.75	36.69	40.22	26.18
	MIROC5	13.15	-15.29	30.81	37.88	22.69	31.91
Annual	MPI-ESM-LR	-22.52	-6.70	45.53	44.54	34.80	31.87
	MME	-8.56	-14.64	28.58	42.04	22.15	32.48
	CM5A-MR	-3.49	-11.53	11.07	17.85	9.11	14.46
	CSIRO	20.94	-1.37	22.94	13.29	20.56	9.55
	EC-EARTH	-6.14	1.38	12.68	15.36	10.64	11.07
	MIROC5	10.59	-11.21	15.77	19.05	12.23	16.00
	MPI-ESM-LR	-1.58	-8.93	8.92	14.99	6.66	11.14
	MME	3.89	-9.60	9.23	16.09	7.04	12.89

298 \*Bold values denotes models that exhibited notable improvements  
 299

300

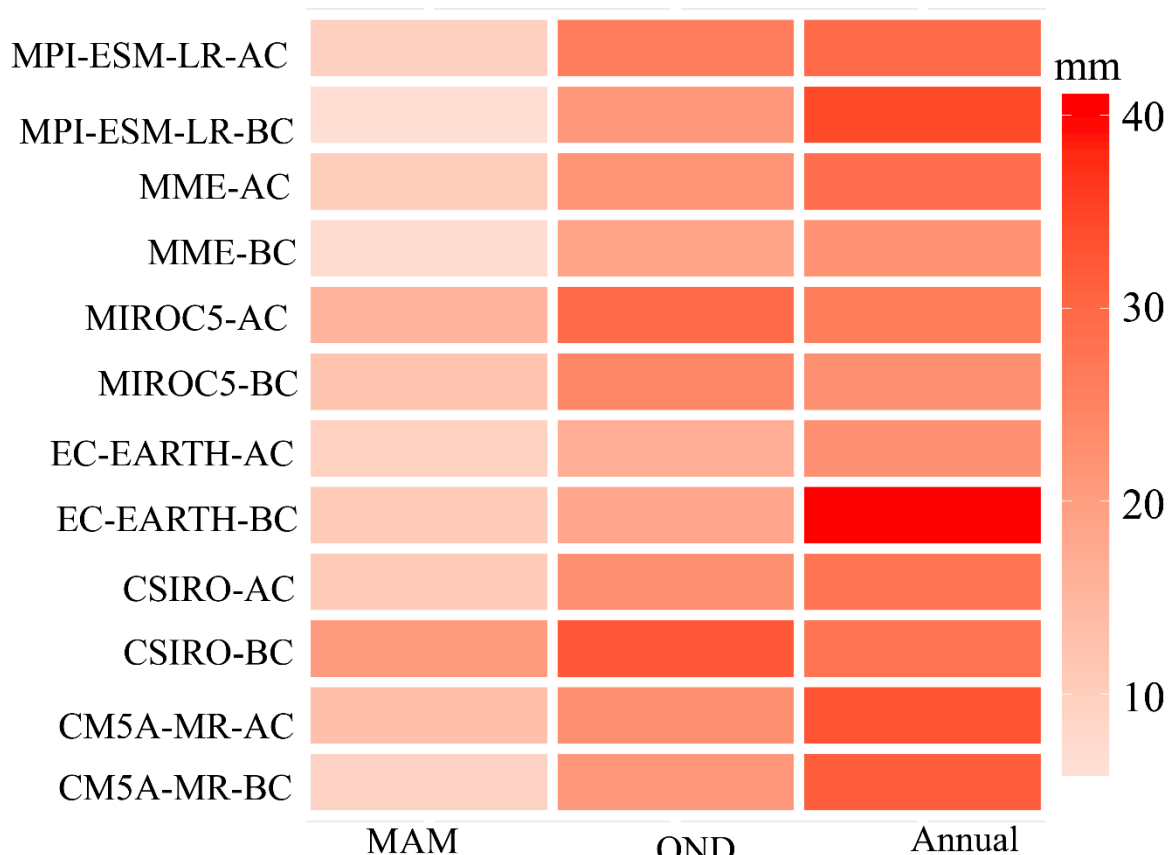
301 This concurs with a study [Kimani et al. \(2018b\)](#), that similarly observed the bias  
302 dependence on rainfall amounts over larger domain of East Africa using satellite derived  
303 precipitation estimates. In fact, [Eden et al. \(2012\)](#) and, [Cannon et al. \(2015\)](#) demonstrated that  
304 persistent biases even after model corrections are as a result of systematic errors in model  
305 outputs from diverse sources. For instance, these studies reported that biases field observed  
306 are originating from either unrealistic response to climate forcing or unpredictable internal  
307 variability that differs from observations. Hence, such biases cannot be corrected by most  
308 correction algorithms. The conclusions from these studies highlighted that only errors in  
309 convective parameterizations and unresolved sub grid-scale orography can be corrected using  
310 univariate statistical bias correction techniques like QMBC employed in the present study.

311 Nevertheless, [Teng et al. \(2015\)](#) proposed a mitigation measure of enhancing the  
312 quality of the datasets that could not be corrected on first attempt by further calibrating the  
313 post processing corrections on adequately long historical records.

314 Further analysis of model bias correction at annual level (**Figure 4e-f**) show  
315 upgrading of most models, most specially the EC-EARTH and CSIRO. However, despite the  
316 corrected model, underestimation of annual rainfall continues to persist even in the corrected  
317 model output. The performance of the algorithm in enhancing the quality of model data  
318 affirms the view of [Ehret et al. \(2012\)](#). To illustrate this view, the study pointed out the  
319 possibility of less value added to models after corrections in situations of complex modelling  
320 chain when considering other sources of uncertainties ([Muerth et al., 2013](#)). The persistent  
321 biases in **Figure 4e-f** (AC) could be associated with dry biases, originating from the ASAL  
322 regions, characterized by moisture outflow over the study region ([Kisembe et al., 2018](#);  
323 [Ayugi et al., 2020](#)). In addition, the high underestimation of wet season (MAM), could have  
324 contributed to overall underestimation of annual rainfall, despite the correction.

325 A summary of performance of bias correction method during the wet season and  
326 annual is shown in **Figure 5**. As noted earlier, most models show improvement after  
327 correction across the diverse timescales. For instance, significant improvement is exhibited  
328 during MAM season as compared to OND. It is worth noting that CM5A-MR had least  
329 improvement during the OND, while substantial improvement is demonstrated by EC-  
330 EARTH during similar season. This confirms the need to improve the models before  
331 employing them for climate change impact studies ([Sillmann et al., 2013](#)).

332



333  
334  
335  
336  
337  
338

**Fig. 5** Heat plot of seasonal and annual Mean Absolute Error (MAE) relative to each model during (1980-2005). A lighter color denotes better results whilst deep color represents unsatisfactory biased corrected value during the wet season and yearly basis.

339 *3.1.2 Spatial bias correction estimates*

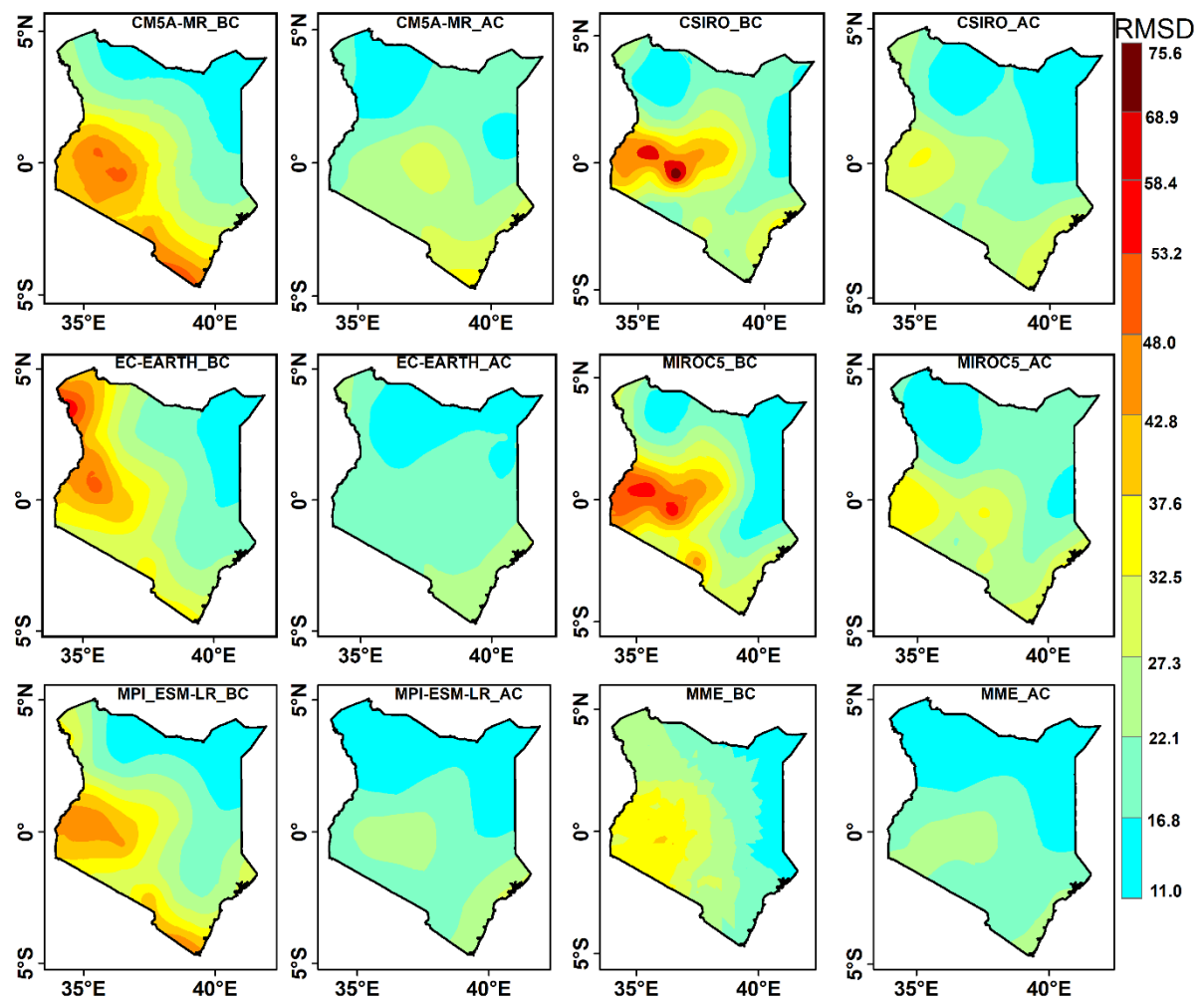
340 **Figure 6** presents spatial patterns of mean annual root mean square difference (RMSD)  
341 during the period 1980-2005 derived from five RCMs as well as their ensemble average. Also  
342 shown in the plots are corresponding bias corrected (abbreviated as AC) RCMs from Rossby  
343 Centre Regional Climate Model (RCA4), as well as the corrected multi model ensemble  
344 (MME). The models were corrected relative to climatic research unit (CRU TS4.02) datasets.  
345 The spatial plots depict regions of underestimations and overestimations and respective areas  
346 of enhancement after employment of quantile mapping technique.

347 It is apparent that significant biases simulated by the models corresponded with the  
348 regions that experience highest rainfall amount. This agrees with observed west to east  
349 gradient demonstrating heavier to lighter rainfall events over the study domain (Kimani et al.,  
350 2018a; Ayugi et al., 2019). As a result, the highest RMSD is noted in central and western  
351 sections of the study area whilst lowest biases (< 22.1 mm/month) is exhibited in the eastern

352 and north western areas. The observed values of RMSD are mostly as a result of complex  
 353 terrains such as high-altitude topographies. The central and western parts of Kenya has a  
 354 varying topography explained by the presence of mountains like Mount Kenya and Mount  
 355 Elgon, respectively. The areas are generally wet and humid, explained by large water bodies  
 356 notable Lake Victoria.

357 As result, most models exhibited satisfactory performance after corrections with EC-  
 358 EARTH, MPI-ESM-LR, and MME demonstrating exemplary improvement as compared to  
 359 other models. The results concur with recent study that noted linear relationship between  
 360 increased rainfall values and subsequent increase of systematic uncertainties (Kimani et al.,  
 361 2018b). The overall monthly reduction in RMSD after correction ranged between 27  
 362 mm/month < RMSD < 11.0 mm/month.

363



364

365 **Figure 6.** Spatial pattern of mean annual RMSD (before correction [BC] and after correction [AC]  
366 for five global climate models (GCMs) dynamically downscaled with the Rossby Centre Regional  
367 Climate Model (RCA4), as well as their ensemble average.

368

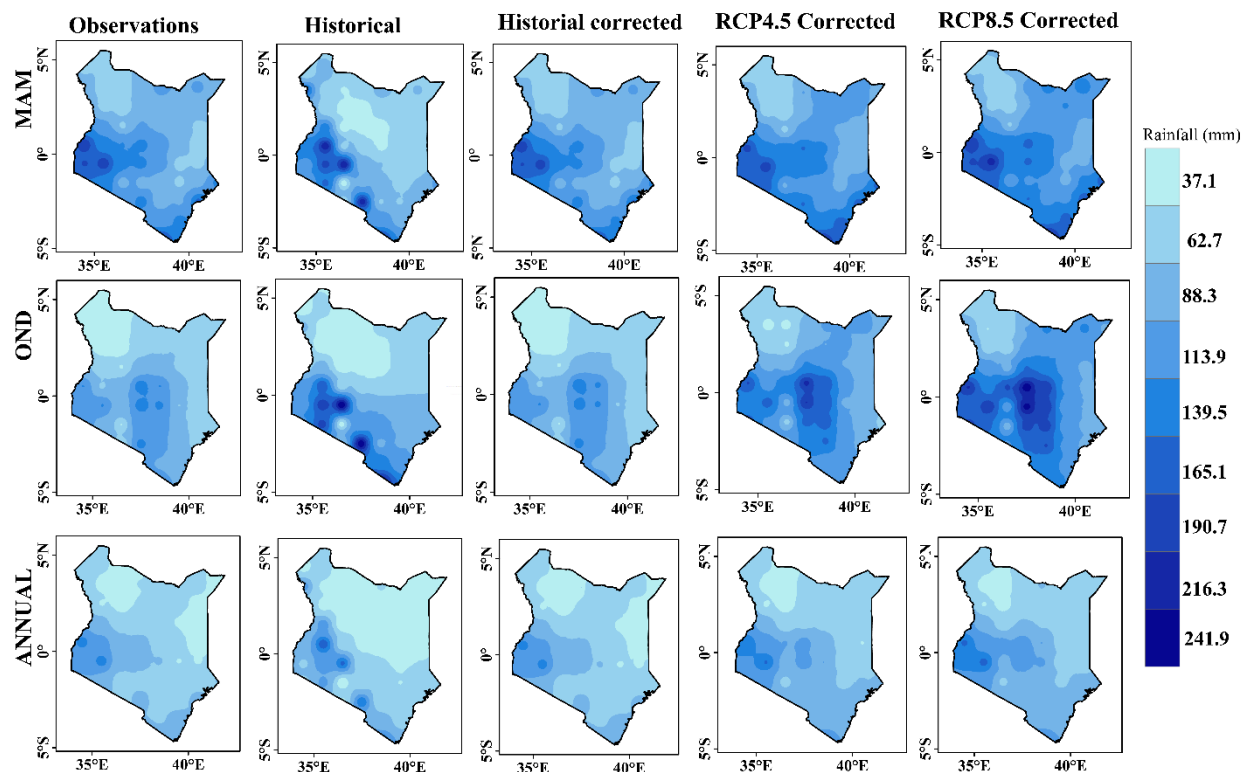
369 Further analysis was conducted in an effort to evaluate how correction algorithm  
370 improves the model projections under RCP4.5 ‘stabilization scenario’ and RCP8.5 ‘business  
371 as usual scenario’. **Figure 7** provides spatial patterns of mean rainfall for seasonal and annual  
372 based on Multi-model ensemble (MME) of five RCMs. The model’s simulations were  
373 corrected using observed data while model projections entailed the simulations and  
374 observations as an input variable. It is apparent that historical simulations after corrections  
375 improved remarkably across various timescales to resemble the spatial patterns of observed  
376 data. Systematic biases appeared to reduce in regions that depicted strong biases, especially  
377 during the MAM rainfall season. Moreover, there was a strong evidence of improvement in  
378 both projections under medium emissions and strong emission scenarios in all the seasons.  
379 However, the regions characterized by complex topography tend to exhibit unsatisfactory  
380 reductions in biases, especially during the OND seasons. For instance, the model corrected  
381 under RCP8.5 depicts strong wet biases over central and western regions as compared to  
382 other timescales. Interestingly, the algorithm tends to show robust performance during the  
383 mean annual cycle that exhibits reduced rainfall occurrence.

384 These results agree with recent reports over broader study domains that have showed  
385 decreasing trends in rainfall patterns towards the end of twentieth century (Yang et al., 2015;  
386 Ongoma and Chen, 2017; Ayugi et al., 2018; Mumo et al., 2019). Further, these studies  
387 demonstrate a continued declining annual rainfall trends for different future scenarios over  
388 the study domain (Rowell et al., 2015; Tierney et al., 2015; Ongoma et al., 2018). On the  
389 contrary, the observed increment patterns during OND season concur with studies that have  
390 reported overestimations of OND, also referred as ‘short rains’ over the study region  
391 (Shongwe et al., 2011; Liebmann et al., 2014; Ongoma et al., 2018). Yang et al. (2015)  
392 highlighted the aspect of challenges associated with simulations of atmosphere-ocean-  
393 monsoon interaction over East Africa region as the major cause of observed bias in models  
394 during OND and MAM projections. According to Liebmann et al. (2014), the warming of  
395 western Indian Ocean continues to play a significant role in simulated and projected patterns  
396 during seasonal rainfall cycle

397 These results clearly depict that the QMBC can satisfactorily improve the models  
398 under different scenarios and timescales hence its relevance for correcting RCMs outputs. Its

399 application will in effect minimize possible biases, therefore it is suitable for evaluation of  
 400 extreme events such as drought and flood that continue to pose threat to livelihoods and  
 401 socio-economic infrastructure over the study domain. Teleconnection patterns responsible for  
 402 influencing the rainfall during the OND is likely to be amplified during the business as usual  
 403 model. This scenario could explain the systematic biases that are persistent in models even  
 404 after the corrections. This calls for a cautious view of the possible limitations of correction  
 405 techniques during the future projections (Cannon et al., 2015).

406



407

408 **Figure 7.** Spatial pattern of mean rainfall for seasonal and annual for observation, simulated,  
 409 simulated corrected and model corrected projections based on MME of 5 global climate models  
 410 (GCMs) dynamically downscaled with the Rossby Centre Regional Climate Model (RCA4).

411

#### 412 4. Conclusion and Recommendation

413 The current study examined the effectiveness of quantile mapping bias correction on Rossby  
 414 Climate Models (RCA4) for drought and flood analysis. The study is a follow-up study by  
 415 Ayugi et al., (2020) on the recent assessment of performance of RCA4 models over the study  
 416 domain. Ayugi et al., (2020) elucidated existence of unsystematic and systematic biases in the  
 417 better performing models across the region. Thus, the current study was conducted within this

418 backdrop. Correction to both mean annual and seasonal variance was conducted by  
419 employing The Split Sample Testing (SST) approach. The correction was conducted by first  
420 training data for 29 years (1951-1979) to derive biases field for monthly averages in model  
421 and observed precipitation simulations. The monthly biased field were then used to correct  
422 independent RCMs during the next 26-year (1980-2005) validation period. The models  
423 corrected are as follows: MIROC5, CSIRO, IPSL-CM5A-MR, MPI-ESM-LR, EC-EARTH,  
424 and MME. Broadly, RCMs simulations depicts significant biases that are mostly associated  
425 with regions of complex terrains such as high altitude or wet humid regions within the study  
426 area. The QMBC demonstrates varying performance from one model to another on both  
427 spatial and temporal scales. However, most models exhibit significant improvement after  
428 corrections on both seasonal and annual timescales. Specifically, the models EC-EARTH and  
429 CSIRO portray exemplary improvement as compared to other models. On the other hand, the  
430 model CM5A-MR model show weak enhancement across various timescales. i.e. MAM and  
431 OND. The corrected models can be employed for projections of extreme events; drought and  
432 flood over the study area. The outputs will aid in appropriate policy formulation for effective  
433 and reliable adaptation techniques. The models showing persistent unsatisfactory  
434 improvement after employing correction approaches should utilized with caution due to the  
435 existence of hidden non-linearity and complex dynamical processes that are uncorrectable.

#### 436 **Acknowledgments**

437 The authors acknowledge Nanjing University of Information Science and Technology  
438 (NUIST) for providing favorable environment and infrastructural needs for conducting  
439 research. National Key Research and Development Program of China  
440 (2018YFC1507703&2016YFA0600702), National Natural Science Foundation of China  
441 (41575070 and 41575085) supported this work. Special appreciation to all data centers for  
442 availing data for the evaluation studies. The lead author is grateful to NUIST for granting him  
443 scholarship to pursue a PhD degree.

#### 444 **Compliance with ethical standards**

445 In a unanimous agreement, all authors declare no conflict of interest in the study.

#### 446 **References**

447 Ahmed, K.F., Wang, G., Silander, J., Wilson, A.M., Allen, J.M., Horton, R., Anyah, R.2013.  
448 Statistical Downscaling and Bias Correction of Climate Model Outputs for Climate  
449 Change Impact Assessment in the U.S. Northeast. Global and Planet. Change 100: 320–

450 32. <http://dx.doi.org/10.1016/j.gloplacha.2012.11.003>.

451 Allen, M.R., Kettleborough, J.A., Stainforth, D.A., 2006. Model error in weather and climate  
452 forecasting. In ECMWF Predictability of Weather and Climate Seminar. European  
453 Centre for Medium Range Weather Forecasts, Reading, UK, <http://www.ecmwf.int/publications/library/do/references/list/209>.

454 Ayugi, B.O., Wen, W., Chepkemoi, D., 2016. Analysis of Spatial and Temporal Patterns of  
455 Rainfall Variations over Kenya. *J. Environ. Earth Sci.*, 6(11).

456 Ayugi, B.O., Tan, G., Ongoma, V., Mafuru, K.B. 2018. Circulations Associated with  
457 Variations in Boreal Spring Rainfall over Kenya. *Earth Syst Environ.* 2, 421–434.  
458 <https://doi.org/10.1007/s41748-018-0074-6>

459 Ayugi BO, Tan G (2019) Recent trends of surface air temperatures over Kenya from 1971 to  
460 2010. *Meteorol. Atmos. Phys.*, 131, 1401-1413 <https://doi.org/10.1007/s00703-018-0644-z>

461 Ayugi, B., Tan, G., Ullah, W., Boiyo, R., Ongoma, V., 2019. Inter-comparison of remotely  
462 sensed precipitation datasets over Kenya during 1998–2016. *Atmos. Res.* 225 (1), 96–  
463 109.<https://doi.org/10.1016/j.atmosres.2019.03.032>

464 Ayugi, B., Tan, G., Gnitou, G.T., Ojara, M., Ongoma, V., 2020. Historical evaluations and  
465 simulations of precipitation over Eastern Africa from Rossby Centre Regional Climate  
466 Model. *Atmos. Res.* 232. <https://doi.org/10.1016/j.atmosres.2019.104705>

467 Block, P.J., Souza Filho, F.A., Sun, L., Kwon, H.H., 2009. A streamflow forecasting  
468 framework using multiple climate and hydrological models 1. *JAWRA*, 45(4), 828-843.  
469 doi:10.1111/j.1752-1688.2009.00327.x

470 Boé, J., Terray, L., Habets, F. and Martin, E., 2007 Statistical and dynamical downscaling of  
471 the Seine Basin climate for hydro-meteorological studies. *Int. J. Climatol.* 27(12), 1643–  
472 1655. <https://doi.org/10.1002/joc.1602>.

473 Bowden, R. (2007). Kenya, 2<sup>nd</sup> edition. Evan Brothers, London, UK.

474 Camberlin, P., Okoola, R.E., 2003. The onset and cessation of the “long rains” in eastern  
475 Africa and their interannual variability. *Theor. Appl. Climatol.*, 54(1–2), 43–54.  
476 <https://doi.org/10.1007/s00704-002-0721-5>.

477 Cannon, A.J., Sobie, S.R., Murdock, T.Q., 2015. Bias correction of GCM precipitation by  
478 quantile mapping: How well do methods preserve changes in quantiles and extremes?. *J. Climate*, 28(17), 6938-6959. <https://doi.org/10.1175/JCLI-D-14-00754.1>

479 Cardell, M.F., R. Romero, A. Amengual, V. Homar, and C. Ramis. 2019. “A Quantile–  
480 Quantile Adjustment of the EURO-CORDEX Projections for Temperatures and  
481 Precipitation.” *Int. J. Climatol.* 39(6):2901–18. <https://doi.org/10.1002/joc/5991>

482 Chen, J., Brissette, F.P., Chaumont, D., Braun, M., 2013. Finding appropriate bias correction  
483 methods in downscaling precipitation for hydrologic impact studies over North  
484 America. *Water Resour. Res.*, 49(7), 4187-4205. <https://doi.org/10.1002/wrcr.20331>

485 Christensen, J. H., Boberg, F., Christensen, O.B., and Lucas P. P.,2008. On the need for bias  
486 correction of regional climate change projections of temperature and precipitation,  
487 *Geophys. Res. Lett.*, 35, L20709, <https://doi.org/10.1029/2008GL035694>.

488 Coron, L., Andreassian, V., Perrin, C., Lerat, J., Vaze, J., Bourqui, M., Hendrickx, F., 2012.  
489 Crash testing hydrological models in contrasted climate conditions: An experiment on  
490 216 Australian catchments. *Water Resour. Res.*, 48(5). doi.org/10.1029/2011WR011721

491 Endris, H.S., Omondi, P., Jain, S., Lennard, C., Hewitson, B., Chang'a, L., Awange, J.L., Dosio, A., Ketiem, P., Nikulin, G., Panitz, H.J., Büchner, M., Stordal, F., Tazalika, L., 2013. Assessment of the performance of CORDEX regional climate models in  
492 simulating East African rainfall. *J. Climate* 26, 8453–8475. <https://doi:10.1175/JCLI-D-12-00708.1>

493 Eden, J.M., Widmann, M., Grawe, D., Rast, S., 2012: Skill, correction, and downscaling of  
494

500 GCM-simulated precipitation. *J. Climate*, 25, 3970–3984, doi:10.1175/JCLI-D-11-  
501 00254.1.

502 Ehret, U., Zehe, E., Wulfmeyer, V., Warrach-Sagi, K., and Liebert, J., 2012. HESS Opinions  
503 “Should we apply bias correction to global and regional climate model data?,” *Hydrol.*  
504 *Earth Syst. Sci.*, 16, 3391–3404, doi:10.5194/hess-16-3391-2012

505 Fang, G., Yang, J., Chen, Y. N., Zammit, C., 2015. Comparing bias correction methods in  
506 downscaling meteorological variables for a hydrologic impact study in an arid area in  
507 China. *Hydrol. Earth Syst. Sci.*, 19(6), 2547-2559. <https://doi:10.5194/hess-19-2547-2015>.

508 FAO., 2019. The state of Food Security and Nutrition in the World 2019. Safeguarding  
509 against economic slowdowns and downturns. Rome, FAO. Licence: CC BY-NC-SA. 3.0  
510 IGO

511 Gudmundsson, L., Bremnes, J.B. Haugen, J.E., Engen-Skaugen, T.2012. “Technical Note:  
512 Downscaling RCM Precipitation to the Station Scale Using Statistical Transformations –  
513 a Comparison of Methods.” *Hydrol. Earth Syst. Sci.*, 16 (9): 3383–90.  
514 <https://doi.org/10.5194/hess-16-3383-2012>.

515 Hastenrath, S., Polzin, D., Mutai, C., 2011. Circulation mechanisms of kenya rainfall  
516 anomalies. *J. Climate* 24(2), 404–412. <https://doi.org/10.1175/2010JCLI3599.1>

517 Harris, I., Jones, P.D., Osborn, T.J., Lister, D.H., 2014. Updated high-resolution grids of  
518 monthly climatic observations – the CRU TS3.10 Dataset. *Int. J. Climatol.*,34: 623–642.  
519 <https://doi.org/10.1002/joc.3711>

520 Hempel, S., Frieler, K., Warszawski, L., Schewe, J., Piontek, F., 2013. A trend-preserving  
521 bias correction—the ISI-MIP approach. *Earth Syst Dynam*, 4(2), 219–  
522 236. <https://doi.org/10.5194/esd-4-219-2013>.

523 Ines, A. V., Hansen, J.W., 2006. Bias correction of daily GCM rainfall for crop simulation  
524 studies. *Agric. Forest.Meteorol.*, 138(1-4), 44-53. <https://doi.org/10.1016/j.agrformet.2006.03.009>

525 IPCC, 2014. Climate Change 2014: Synthesis Report. Contribution of Working Groups I, II  
526 and III to the Fifth Assessment Report of the Intergovernmental Panel on Climate  
527 Change [Pachauri RK, Meyer LA (eds.)]. IPCC, Geneva, Switzerland, 151 pp.

528 Klemeš, V., 1986. Operational testing of hydrological simulation models. *Hydrolog.Sci.*  
529 J., 31(1), 13-24. <https://doi.org/10.1080/0262666860941024>

530 Kimani, M. W., Hoedjes, J. C. B., Su, Z., 2018a. An assessment of satellite-derived rainfall  
531 products relative to ground observations over East Africa. *Remote Sens*, 9(5). 430.  
532 <https://doi.org/10.3390/rs9050430>

533 Kimani, M., Hoedjes, J., Su, Z., 2018b. Bayesian Bias Correction of Satellite Rainfall  
534 Estimates for Climate Studies. *Remote Sens*, 10(7), 1074. <https://doi.org/10.3390/rs10071074>

535 Kisembe, J., Favre, A., Dosio, A., Lennard, L., Sabiiti, G., Nimusiuma, A., 2018. Evaluation  
536 of rainfall simulations over Uganda in CORDEX regional climate models. *Theor. Appl.*  
537 *Climatol.* 137(1-2), 1117–1134. <https://doi.org/10.1007/s00704-018-2643-x>

538 King'uyu, S.M, Ogallo, L.A, Anyamba, E.K., 2000. Recent Trends of Minimum and  
539 Maximum Surface Temperatures over Eastern Africa. *J Climate* 13: 2876–2886.  
540 <https://doi.org/10.1175/1520-0442-13-2876-Kinguyu>

541 Kotttek, M., Grieser, J., Beck, C., Rudolf, B., Rubel, F., 2006. World map of the Köppen-  
542 Geiger climate classification updated. *Meteorologische Zeitschrift*, 15(3), 259–263.  
543 <https://doi.org/10.1127/0941-2948/2006/0130>

544 Leander, R., Buishand, T.A., 2007. Resampling of regional climate model output for the  
545 simulation of extreme river flows. *J. Hydrol.*, 332(3-4), 487–  
546 496. <https://doi.org/10.1016/j.jhydrol.2006.08.0076>

547 Leander, R., Buishand, T.A., van den Hurk, B.J., de Wit, M. J., 2008. Estimated changes in  
548 flood quantiles of the river Meuse from resampling of regional climate model output. *J.*  
549 *Hydrol.*, 351(3-4), 331-343. <https://doi.org/10.1016/j.jhydrol.2007.12.020>.

550 550 551 552 553 554 555 556 557 558 559 560 561 562 563 564 565 566 567 568 569 570 571 572 573 574 575 576 577 578 579 580 581 582 583 584 585 586 587 588 589 590 591 592 593 594 595 596 597 598 599

Lenderink, G., Buishand, A., Deursen, W.V., 2007. Estimates of future discharges of the river Rhine using two scenario methodologies: direct versus delta approach. *Hydrol. Earth Syst. Sci.* 11(3), 1145-1159. doi:10.5194/hess-11-1145-2007

Li, C.Z., Zhang, L., Wang, H., Zhang, Y.Q., Yu, F.L., Yan, D.H., 2012. The transferability of hydrological models under nonstationary climatic conditions. *Hydrol. Earth Syst. Sci.*, 16(4), 1239-1254. doi:10.5194/hess-16-1239-2012

Liebmann, B., Hoerling M.P., Funk, C., Bladé, I., Dole, R.M., Allured, D., Quan, X., Pegion P., Eischeid, J.K., 2014. Understanding Recent Eastern Horn of Africa Rainfall Variability and Change. *J. Climate*, 27: 8630–8645. doi:10.1175/JCLI-D-13-00714.1

Malhi, Y., Wright, J., 2004. Spatial patterns and recent trends in the climate of tropical rainforest regions. *Phil. Trans. R. Soc. Lond. B*, 359(1443), 311-329. doi:10.1098/rstb.2003.1433

Maraun, D., 2013. Bias correction, quantile mapping, and downscaling: Revisiting the inflation issue. *J. Climate*, 26(6), 2137-2143. doi:10.1175/JCLI-D-12-00821.1

Maraun, D., 2012: Nonstationarities of regional climate model biases in European seasonal mean temperature and precipitation sums. *Geophys. Res. Lett.*, 39, L06706, doi:10.1029/2012GL051210

Mearns, L.O., Arritt, R., Binner, S., Bukovsky, S.M., McGinnis, S., Sain, S., Caya, D., Correia, J., Flory, D., Gutowski, W., Takle, E.S., Jones, R., Leung, R., Okia, M.W., McDaniel, L., Nunes, A.M.B., Qian, Y., Roads, J., Sloan, L., Snyder, M., 2012: The North American Regional Climate Change Assessment Program: Overview of phase I results. *Bull. Amer. Meteor. Soc.*, 93, 1337–1362, doi:10.1175/BAMS-D-11-00223.1

Maraun, D., Wetterhall, F., Ireson, A. M., Chandler, R. E., Kendon, E. J., Widmann, M., Brien, S., Rust, H. W., Sauter, T., Themeßl, M., Venema, V. K. C., Chun, K. P., Goodess, C. M., Jones, R. G., Onof, C., Vrac, M., and Thiele-Eich, I., 2010. Precipitation downscaling under climate change: Recent developments to bridge the gap between dynamical models and the end user, *Rev. Geophys.*, 48, RG3003, doi:10.1029/2009RG000314.

Maurer, E. P., Pierce, D. W., 2014. Bias correction can modify climate model simulated precipitation changes without adverse effect on the ensemble mean. *Hydrol. Earth Syst. Sci.*, 18(3), 915-925. doi:10.5194/hess-18-915-2014

Muerth, M. J., Gauvin St-Denis, B., Ricard, S., Velázquez, J.A., Schmid, J., Minville, M., Caya, D., Chaumont, D., Ludwig, R., and Turcotte, R., 2013. On the need for bias correction in regional climate scenarios to assess climate change impacts on river runoff, *Hydrol. Earth Syst. Sci.*, 17, 1189–1204, doi:10.5194/hess-17-1189-2013.

Moore, K., Pierson, D., Pettersson, K., Schneiderman, E., Samuelsson, P., 2008. Effects of warmer world scenarios on hydrologic inputs to Lake Mälaren, Sweden and implications for nutrient loads. *Hydrobiologia*, 599:191-199, doi:10.1007/s10750-007-9197-8

Mumo, L., Yu, J., Fang, K., 2018. Assessing Impacts of Seasonal Climate Variability on Maize Yield in Kenya. *Int. J. Plant Prod.* 12, 1-11. doi:10.1007/s42106-018-0027-x.

Mumo, L., Yu, J., Ayugi, B., 2019. Evaluation of spatiotemporal variability of rainfall over Kenya from 1979 to 2017. *J. Atmospheric Sol-Terr. Phys.*, 194, 105097. <https://doi.org/10.1016/j.jastp.2019.105097>.

Murphy, J., 1999. An evaluation of statistical and dynamical techniques for downscaling local climate. *J. Climate*, 12, 2256-2284.

Nicholson, S.E., 2008. The intensity, location and structure of the tropical rainbelt over west Africa as factors in interannual variability. *Int. J. Climatol.* 128, 1775–1785. <https://doi.org/10.1002/joc.1507>.

Nicholson, S.E., 2017. Climate and climatic variability of rainfall over eastern Africa. *Rev. Geophys.* 55, 590–635. <https://doi.org/10.1002/2016RG000544>

600 Ogwang, B.A, Chen, H., Li, X., Gao, C., 2014. The Influence of Topography on East African  
601 October to December Climate: Sensitivity Experiments with RegCM4. *Adv. Meteorol.*  
602 2014. ID 143917. <https://doi.org/10.1155/2014/143917>

603 Ongoma, V., Chen, H., Gao, C., Sagero, P.O., 2017. Variability of temperature properties over  
604 Kenya based on observed and reanalyzed datasets. *Theor. Appl. Climatol.* 133:1175-  
605 1190. <http://doi.org/10.1007/s00704-017-2246-y>

606 Ongoma, V., Chen, H., 2017. Temporal and spatial variability of temperature and precipitation  
607 over East Africa from 1951 to 2010. *Meteorol. Atmos. Phys.*, 129(2) 131-144.  
608 <http://doi.org/10.1007/s00703-016-0462-0>.

609 Ongoma, V., Chen, H., Gao, C., 2018. Projected Change in Mean Rainfall and Temperature  
610 over East Africa based on CMIP5 Models. *Int. J. Climatol.* 38: 1375-1392  
611 <https://doi.org/10.1002/joc.5252>

612 Ongoma, V., Chen, H., Gao, C., 2019. Evaluation of CMIP5 twentieth century rainfall  
613 simulation over the equatorial East Africa. *Theor. Appl. Climatol.* 135 (3-4), 893-910.  
614 <http://doi.org/10.1007/s00704-018-2392-x>

615 Panofsky, H.A., Brier, G.W., 1968. Some Application of Statistics to  
616 Meteorology, 224 pp., Pa. State Univ., University Park, Pa

617 Piani, C., Haerter, J. O., Coppola, E., 2009. Statistical bias correction for daily precipitation  
618 in regional climate models over Europe. *Theor. Applied Climatol.* 99(1-2), 187-  
619 192. doi:10.1007/s00704-009-0134-9

620 Samuelsson, P., Jones, C.G., Willén, U., Ullerstig, A., Gollvik, S., Hansson, U., Hansson, U.,  
621 Jansson, C., Kjellström, E., Nikulin, G., Wyser, K., 2012. The Rossby Centre regional  
622 climate model RCA3: model description and performance. *Tellus A* 63, 4-23.  
623 <https://doi:10.1111/j.1600-0870.2010.00478.x>

624 Schmidli, J., Frei, C., Vidale, P. L., 2006. Downscaling from GCM precipitation: a  
625 benchmark for dynamical and statistical downscaling methods. *Int. J. Climatol.*, 26(5),  
626 679-689. doi:10.1002/joc.1287

627 Sillmann, J., Kharin, V., Zhang, X., Zwiers, F., Branaugh, D., 2013: Climate extremes  
628 indices in the CMIP5 multimodel ensemble: Part 1. Model evaluation in the present  
629 climate. *J. Geophys. Res. Atmos.*, 118, 1716-1733, doi:10.1002/jgrd.50203.

630 Sun, F., Roderick, M. L., Lim, W. H., Farquhar, G.D., 2011. Hydroclimatic projections for  
631 the Murray-Darling Basin based on an ensemble derived from Intergovernmental Panel  
632 on Climate Change AR4 climate models. *Water Resour. Res.* 47(12). doi:10.1029/2010WR009829

634 Shongwe, M.E, Van Oldenborgh, G.J, Van den Hurk, B, Van Aalst M., 2011. Projected  
635 changes in mean and extreme precipitation in Africa under global warming. Part II: East  
636 Africa. *J Climate* 24: 3718-3733. <http://doi.org/10.1175/2010JCLI2883.1>.

637 Strandberg, G., Bärring, L., Hansson, U., Jansson, C., Jones, C., Kjellström, E., Kupiainen,  
638 M., Nikulin, G., Samuelsson, P., Ullerstig, A., 2014. CORDEX scenarios for Europe  
639 from the Rossby Centre regional climate model RCA4. Technical report 116, Climate  
640 research Rossby Centre.

641 Rasmussen, J., Sonnenborg, T.O., Stisen, S., Seaby, L. P., Christensen, B.S., Hinsby, K.,  
642 2012. Climate change effects on irrigation demands and minimum stream discharge:  
643 impact of bias-correction method. *Hydrol. Earth Syst. Sci.*, 16(12), 4675-  
644 4691. doi:10.5194/hess-16-4675-2012

645 Rojas, R., Feyen, L., Dosio, A., Bavera, D., 2011. Improving pan-European hydrological  
646 simulation of extreme events through statistical bias correction of RCM-driven climate  
647 simulations. *Hydrol. Earth Syst. Sci.*, 15(8). doi:10.5194/hess-15-2599-2011

648 Rowell, D.P., Booth, B.B.B., Nicholson, S.E., Good, P., 2015. Reconciling past and future

649 rainfall trends over East Africa. *J. Climate* 28 (24), 9768–9788.  
650 <https://doi.org/10.1175/JCLI-D-15-0140.1>

651 Teutschbein, C., and Seibert, J., 2010. Regional climate models for hydrological impact  
652 studies at the catchment scale: a review of recent modeling strategies. *Geogr. Comp.*, 4(7),  
653 834–860. doi:10.1111/j.1749-8198.2010.00357.x

654 Teutschbein, C., and J. Seibert, 2012: Bias correction of regional climate model simulations  
655 for hydrological climate-change impact studies: Review and evaluation of different  
656 methods. *J. Hydrol.*, 456–457, 12–29, doi:10.1016/j.jhydrol.2012.05.052.

657 Teutschbein, C., Seibert, J., 2013. Is bias correction of regional climate model (RCM)  
658 simulations possible for non-stationary conditions?. *Hydrol. Earth Syst. Sci.*, 17(12),  
659 5061–5077. doi:10.51194/hess-17-5061-2013

660 Teng, J., N. Potter, F. Chiew, L. Zhang, B. Wang, J. Vaze, and J. Evans, 2015: How does bias  
661 correction of regional climate model precipitation affect modelled runoff? *Hydrol. Earth  
662 Syst. Sci.*, 19, 711–728, doi:10.51194/hess-19-711-2015

663 Tierney, J.E., Ummenhofer, C.C., deMenocal, P.B., 2015. Past and future rainfall in the Horn  
664 of Africa. *Sci. Adv.*, 1(9), e1500682. <https://doi:10.1126/sciadv.1500682>

665 Tramblay, Y., Ruelland, D., Somot, S., Bouaicha, R., Servat, E., 2013. High-resolution Med-  
666 CORDEX regional climate model simulations for hydrological impact studies: a first  
667 evaluation of the ALADIN-Climate model in Morocco. *Hydrol. Earth Syst. Sci.*, 17(10).doi:10.51194/hess-17-3721-2013

669 Terink, W., Hurkmans, R. T. W. L., Uijlenhoet, R., Warmerdam, P. M. M., Torfs, P.J.J.F.,  
670 2008. Bias correction of temperature and precipitation data for regional climate model  
671 application to the Rhine basin. Wageningen Universiteit.

672 Themeßl, M. J., Gobiet, A., and Leuprecht, A.,2011. Empirical statistical downscaling and  
673 error correction of daily precipitation from regional climate models, *Int. J. Climatol.*, 31,  
674 1530–1544, doi:10.1002/joc.2168.

675 Wilby, R.L., Wigley, T.M.L., 2000. Precipitation predictors for downscaling: observed and  
676 general circulation model relationships. *Int. J. Climatol.* 20(6), 641-661.

677 Wood, A.W., Leung, L.R., Sridhar, V., Lettenmaier, D.P., 2004. Hydrologic implications of  
678 dynamical and statistical approaches to downscaling climate model outputs. *Climatic  
679 change*, 62, 189–216. doi.1023/B:CLIM.0000013685.99609.9e

680 Yang, W., Seager R, Cane M.A, Lyon B., 2015. The annual cycle of East African  
681 precipitation. *J Climate* 28: 2385–2404. doi:10.1175/JCLI-D-14-00484.1.  
682